Transportation Research Part C 118 (2020) 102717

Contents lists available at ScienceDirect

Transportation Research Part C

journal homepage: www.elsevier.com/locate/trc

Distributed model predictive control of multi-vehicle systems with switching communication topologies

Keqiang Li[a], Yougang Bian[a,*], Shengbo Eben Li[a], Biao Xu[b], Jianqiang Wang[a]

[a] State Key Laboratory of Automotive Safety & Energy, School of Vehicle and Mobility, Tsinghua University, Beijing, China
[b] State Key Laboratory of Advanced Design & Manufacturing for Vehicle Body, College of Mechanical and Vehicle Engineering, Hunan University, Changsha, China

ARTICLE INFO

Keywords:
Connected vehicles
Distributed control
Model predictive control
Switching communication topology

ABSTRACT

Vehicle-to-vehicle (V2V) communication-enabled cooperation of multiple connected vehicles improves the safety and efficiency of our transportation systems. However, the joining and leaving of vehicles and unreliability of wireless communication channels will cause the switching of communication topology among vehicles, thus affecting the performance of multi-vehicle systems. To address this issue, a distributed model predictive control (DMPC) method is proposed for multi-vehicle system control under switching communication topologies. First, an open-loop optimization problem is formulated, within which neighbor-deviation and self-deviation penalties and constraints are incorporated to ensure stability. Then, a DMPC algorithm is designed for multi-vehicle systems subject to switching communication topologies. For the closed-loop system, the convergence of predicted terminal states is proved based on the neighbor-deviation constraint. After that, closed-loop system stability is analysed based on a common Lyapunov function (CLF) defined using a joint neighbor set. It is proved that asymptotic stability of the closed-loop system can be achieved through a sufficient condition on the weight matrices of the open-loop optimization problem. Numerical simulations are conducted to demonstrate the effectiveness of the proposed DMPC controller.

1. Introduction

The emerging of vehicle-to-vehicle (V2V) communication technique enables the cooperation of multiple connected vehicles for improved traffic flow stability (Talebpour and Mahmassani, 2016), fuel economy (Xu et al., 2019), traffic throughput (Talebpour and Mahmassani, 2016, 2017, 2019), and travel efficiency (Xu et al., 2018). In a one-dimensional multi-vehicle system, a string of connected vehicles follow a leading vehicle while maintaining a safety inter-vehicle distance, yielding the so-called vehicle platoons. Recent advances in the cooperation of multi-vehicle systems and vehicle platoons can be found in Li et al. (2017), Wang et al. (2020b).

The study of vehicle platoons can date back to the PATH program (Shladover et al., 1991; Shladover, 2007). Up till now, the platoon control technique has attracted a lot of attention. Typical research topics of platoon control include the study of range policies (Darbha and Hedrick, 1999; Zhou and Peng, 2005; Rödönyi, 2018), string stability (Seiler et al., 2004, 2011, 2014, 2018, 2019), dynamics heterogeneity (Wang, 2018; Bian et al., 2019), communication time delays (di Bernardo et al., 2015; di Bernardo

* Corresponding author.
E-mail addresses: likq@tsinghua.edu.cn (K. Li), byg10@foxmail.com (Y. Bian), lishbo@tsinghua.edu.cn (S.E. Li), dr_xubiao@163.com (B. Xu), wjqlws@tsinghua.edu.cn (J. Wang).

https://doi.org/10.1016/j.trc.2020.102717
Received 1 November 2019; Received in revised form 7 May 2020; Accepted 30 June 2020
Available online 01 August 2020

et al., 2016; Zhang and Orosz, 2016; Ge and Orosz, 2017), *etc. The vehicle platoon control technique has also been applied to automated intersection control (*Xu et al., 2018*;* Bian et al., 2019*). In these studies, different control methods have been used to address various control issues. For example, $\mathcal{H}_\infty$ control was used in* Ploeg et al. (2014), Li et al. (2018a) *to achieve disturbance rejection as well as string stability. Distributed adaptive and sliding mode control was used in* Kwon and Chwa (2014), Gao et al. (2018) *to address model uncertainties and external disturbances. Distributed model predictive control (DMPC) was used in* Dunbar and Caveney (2012), Zheng et al. (2017, 2019) *to achieve online trajectory optimization with respect to a pre-designed cost function.*

The studies mentioned above are all based on the assumption of a time-invariant communication topology among vehicles. However, wireless V2V communication is inherently unreliable due to the existence of package losses and channel failures, which will further cause the switching of communication topologies (Wang et al., 2020a). Moreover, the joining and leaving of vehicles from a multi-vehicle system may also cause communication topology switching. By viewing a multi-vehicle system as a switching system that switches among different communication topologies, one can regard each possible communication topology as a specific subsystem mode. As stated in Liberzon (2003), switching actions among even stable subsystems may cause the instability of a closed-loop system. This phenomenon will heavily affect the cooperation performance of multi-vehicle systems.

To address the issue of switching communication topologies, some researchers proposed to optimize the communication topology dynamically considering communication failure possibilities for improved platoon performance (Wang et al., 2020a). Besides online topology optimization, robust controller design considering topology switching also attracts researchers' attention. In this field, one typical approach is the common Lyapunov function (CLF) method. As stated in Liberzon (2003), a system is asymptotic stable under arbitrary switching if there exists a CLF for all of the subsystems. Based on this theorem, a CLF based method was proposed in Chehardoli and Homaeinezhad (2017) for the control of vehicle platoons subject to arbitrary topology switching. In particular, this study requires a globally reachable leader (*i.e.*, there exists a directed spanning tree rooted at the leading vehicle in the communication topology) under all of the possible communication topologies. The study in Salvi et al. (2017) has the same requirement as Chehardoli and Homaeinezhad (2017); however, specific conditions on the in-degree and out-degree of the communication topology among vehicles are also required to be satisfied to guarantee the stability of vehicle platoons. In contrast to these two studies that only require directed communication topologies, the study in Li et al. (2018b) require the switching communication topologies to be undirected so that finite-time stabilization can be achieved for better convergence performance.

The aforementioned studies on switching communication topologies are all based on explicit feedback control. When it comes to DMPC, which relies on online optimization and has the advantage to explicitly address constraints and nonlinearities, there are mainly two approaches to address switching communication topologies: (1) the first approach is based on dynamic weights of cost functions, which will be adjusted as the communication topology switches so that the Lyapunov function is monotonically decreasing, see Ding et al. (2016); (2) the second approach is based on auxiliary constraints, which restrict agents' trajectory deviations when the communication topology switches so that coupled constraint conditions are always satisfied, see Schaich et al. (2014). A combination of these two methods can be found in Wang et al. (2017). Note that both of these two solutions require a fully connected leader (*i.e.*, there exists a directed communication channel from the leader to each of the followers) under all of the possible communication topologies. This requirement is more strict than that of a globally reachable leader under all of the possible communication topologies, thus is difficult to be satisfied in practice. Some studies consider one-step predictive horizon or constraint-free cases, then the control input and closed-loop system can be explicitly derived for system analysis, see Zhan and Li (2013), Cheng et al. (2015). A method to separate system stability and control performance was also proposed in Heidarinejad et al. (2011) to address communication failures.

In order to eliminating the requirement of a globally reachable or fully connected leader under all of the possible communication topologies in the existing studies, this paper proposes a new DMPC method for cooperative control of multi-vehicle systems under switching communication topologies. Compared with the existing studies, the main contribution of this paper includes:

1. By using a neighbor-deviation constraint in the open-loop optimization problem, a sufficient condition is derived to guarantee the convergence of predicted terminal states. This condition extends the requirement of unidirectional topologies in Zheng et al. (2017), where information only flows from preceding vehicles to following ones, to the case of directed and acyclic graphs (DAGs). This condition also helps eliminate the requirement of a globally reachable leader (Chehardoli and Homaeinezhad, 2017; Salvi et al., 2017) or a fully connected leader (Ding et al., 2016; Schaich et al., 2014; Wang et al., 2017) under all of the possible communication topologies.
2. A self-deviation constraint is proposed in the open-loop optimization problem to restrict the expansion of vehicles' deviations between assumed and predicted state trajectories in two successive sampling instants. In addition, a joint-neighbor-set based CLF is proposed for stability analysis of multi-vehicle systems subject to switching communication topologies. Through Lyapunov analysis, a sufficient condition on the weight matrices of the open-loop optimization problem is derived to guarantee asymptotic stability of multi-vehicle systems. This method extends the study of Zheng et al. (2017) to the case of switching communication topologies.

The rest of the paper is organized as follows: Section 2 presents the problem statement of multi-vehicle system control. Section 3 presents the design of the distributed model predictive controller. Section 4 presents stability analysis of the closed-loop system. Simulation results are given in Section 5, and conclusions are drawn in Section 6.

Notations: The fields of integers, real numbers, and $m \times n$ real matrices are denoted by $\mathbb{N}$, $\mathbb{R}$, and $\mathbb{R}^{m\times n}$, respectively. An $mn \times mn$ block diagonal matrix, whose diagonal blocks $M_1, M_2, ..., M_n \in \mathbb{R}^{m\times m}$ start from the upper left, is denoted by $\mathrm{diag}\{M_1, M_2, ..., M_n\}$ for convenience. For any $N \in \mathbb{N}^+$, define $\mathcal{N} := \{1, 2, 3, ..., N\}$. Given a vector $x \in \mathbb{R}^m$ and a positive definite matrix $P \in \mathbb{R}^{m\times m}$, define

$\|x\|_P := \sqrt{x^\top P x}$. Denote by $\otimes$ the Kronecker product, which satisfies $(A \otimes B)\cdot(C \otimes D) = (AC) \otimes (BD)$. Denote by $|\mathbb{S}|$ the cardinality of a set $\mathbb{S}$, and by $\mathbb{S}_1 \backslash \mathbb{S}_2$ the operation of subtracting set $\mathbb{S}_2$ from set $\mathbb{S}_1$. Denote by $y(k|t)$ the future value of $y(k+t)$ predicted at time t. For any $N_p \in \mathbb{N}^+$, define $\mathbb{K}_0 := \{0, 1, 2, ..., N_p - 1\}$ and $\mathbb{K}_1 := \{1, 2, 3, ..., N_p\}$. Given a multivariate function $f(\cdot)$, we abbreviate $f(x_1(k|t), ..., x_m(k|t))$, $f(x_1(0|t), ..., x_1(N_p-1|t), ..., x_m(0|t), ..., x_m(N_p-1|t))$, and $f(x_1(1|t), ..., x_1(N_p|t), ..., x_m(1|t), ..., x_m(N_p|t))$ as $f(x_1, ..., x_m; k|t)$, $f(x_1, ..., x_m; \mathbb{K}_0|t)$, and $f(x_1, ..., x_m; \mathbb{K}_1|t)$, respectively.

Lemma 1 (*Khamsi and Kirk, 2011*). For any vectors $x_1, x_2 \in \mathbb{R}^N$ and positive definite matrix $M \in \mathbb{R}^{N\times N}$, it holds that:

$$\|x_1\|_M + \|x_2\|_M \geqslant \|x_1 + x_2\|_M.$$

Lemma 2 (*Steele, 2004*). For any real numbers $x_1, x_2, ..., x_N \geqslant 0$, it holds that:

$$\left(\sum_{i=1}^{N} x_i\right)^2 \leqslant N \sum_{i=1}^{N} x_i^2.$$

2. Problem Statement

This section details the problem of multi-vehicle system control. Firstly, the longitudinal vehicle dynamic system is presented. After that, the switching communication topology is modeled. Based on these models, the control objective of multi-vehicle systems is finally formulated.

2.1. Longitudinal vehicle dynamics

Consider a group of $N+1$ vehicles with the leading one indexed by 0 and the following ones indexed by $1, 2, ..., N$. The discrete-time dynamics of the leading and following vehicles are:

$$p_i(t+1) = p_i(t) + v_i(t)\Delta t, \tag{1a}$$

$$v_i(t+1) = v_i(t) + a_i(t)\Delta t, \tag{1b}$$

$$a_i(t+1) = a_i(t) + g_i(v_i(t), a_i(t), T_i(t), T_{des,i}(t))\Delta t, \tag{1c}$$

where $i \in \{0\} \cup \mathcal{N}$ is vehicle index, Δt is the sampling time; p_i, v_i, and a_i are the position, velocity, and acceleration, respectively; T_i and $T_{des,i}$ are the actual and desired driving/braking torques, respectively; $g_i(\cdot)$ is given as

$$g_i(v_i(t), a_i(t), T_i(t), T_{des,i}(t)) = \frac{\eta_i}{m_i r_i \tau_i}(T_{des,i}(t) - T_i(t)) - 2\frac{C_{A,i}}{m_i} v_i(t) a_i(t),$$

where m_i and r_i are the vehicle mass and tire radius, respectively; η_i and τ_i are the mechanical efficiency and time lag of the driveline, respectively; $C_{A,i}$, f_i, and g are the coefficients of aerodynamic drag, rolling resistance, and gravitational acceleration, respectively. Note that model (1) is a generalization of the vehicle models used in Xiao and Gao (2011), Zheng et al. (2016).

Define vehicle state $x_i(t) := [p_i(t), v_i(t), a_i(t)]^\top$. By using the exact feedback linearization technique (Xiao and Gao, 2011), we can rewrite model (1) into the following form:

$$x_i(t+1) = Ax_i(t) + Bu_i(t), \tag{2}$$

where

$$A = \begin{bmatrix} 1 & \Delta t & 0 \\ 0 & 1 & \Delta t \\ 0 & 0 & 1 \end{bmatrix}, B = \begin{bmatrix} 0 \\ 0 \\ \Delta t \end{bmatrix},$$

and $u_i(t) = g_i(v_i(t), a_i(t), T_i(t), T_{des,i}(t))$ is the equivalent control input, from which $T_{des,i}(t)$ can be calculated. In fact, $u_i(t)$ can be viewed as an upper control input that is sent to a lower controller $T_{des,i}(t) = g_i^{-1}(v_i(t), a_i(t), T_i(t), u_i(t))$ for actuator control. Here we assume vehicles' control inputs are bounded, *i.e.*,

$$u_i \in \mathcal{U}_i := \{x \in \mathbb{R} \,|\, u_{i,\min} \leqslant x \leqslant u_{i,\max}\},$$

where $u_{i,\min} < 0$ and $u_{i,\max} > 0$ are known constants.

2.2. Switching communication topology

Denote by $\mathcal{G}(t) = \{\mathcal{V}, \mathcal{E}(t), \mathcal{A}(t)\}$ a directed time-varying graph corresponding to following vehicles' communication topology at time t. In $\mathcal{G}(t)$, $\mathcal{V} = \{\mathcal{V}_1, \mathcal{V}_2, ..., \mathcal{V}_N\}$ is the set of N vertices (or following vehicles), $\mathcal{E}(t) \subseteq \mathcal{V} \times \mathcal{V}$ is the set of time-varying edge set, and $\mathcal{A}(t) = [a_{ij}(t)] \in \mathbb{R}^{N\times N}$ is the set of time-varying adjacency matrix. In $\mathcal{A}(t)$, $a_{ij}(t)$ equals 1 if vertex i can obtain the information of vertex j at time t, or 0, otherwise. We assume there is no self-loop in $\mathcal{G}(t)$, *i.e.*, $a_{ij}(t) \neq 0, \forall\, t \geqslant 0$. A directed graph $\mathcal{G}$ is said to contain a spanning tree if there exists a tree-type subgraph of $\mathcal{G}$ that includes all of the vertices of $\mathcal{G}$.

Suppose that $\mathcal{G}(t) \in \mathbb{G} := \{\mathcal{G}_1, \mathcal{G}_2, ..., \mathcal{G}_M\}$, where $M \in \mathbb{N}^+$ is the number of communication topology candidates. Denote by $\mathbb{N}_i(t)$ and $\mathbb{O}_i(t)$ the *in-neighbor set* and *out-neighbor set* of following vehicle i at time t, respectively, *i.e.*,

$$\mathbb{N}_i(t) := \{j \in \mathcal{N}, j \neq i | a_{ij}(t) = 1\},$$
$$\mathbb{O}_i(t) := \{j \in \mathcal{N}, j \neq i | a_{ji}(t) = 1\}.$$

Note that $\mathbb{N}_i(t)$ only contain the indices of following vehicles. To model the communication between the leading vehicle and following vehicles, define a pinning set

$$\mathbb{P}_i(t) := \begin{cases} \{0\}, & \text{if } b_i(t) = 1, \\ \varnothing, & \text{if } b_i(t) = 0, \end{cases}$$

where $b_i(t)$ equals 1 if following vehicle i can obtain the information of the leading vehicle at time t, or 0, otherwise. Further we define a pinning in-neighbor set

$$\mathbb{I}_i(t) := \mathbb{N}_i(t) \bigcup \mathbb{P}_i(t).$$

Finally, the *joint in-neighbor set* and *joint out-neighbor set* are respectively defined as

$$\mathbb{A}_i := \bigcup_{t=0}^{+\infty} \mathbb{I}_i(t),$$
$$\mathbb{B}_i := \bigcup_{t=0}^{+\infty} \mathbb{O}_i(t).$$

A directed graph is called a DAG if it contains no cycles. A DAG has at least one topological sorting, *i.e.*, a linear ordering of vertices such that for every directed edge from $\mathcal{V}_j$ to $\mathcal{V}_i$, vertex $\mathcal{V}_j$ comes before $\mathcal{V}_i$ in the ordering. As shown in Fig. 1, graphs (a)-(c) are DAGs while graph (d) is not, since vertices $\mathcal{V}_1$, $\mathcal{V}_2$, and $\mathcal{V}_3$ and vertices $\mathcal{V}_1$, $\mathcal{V}_4$, and $\mathcal{V}_3$ form two cycles. Moreover, {1, 4, 2, 3} and {1, 2, 4, 3} in graphs (b) and (c) are two topological sortings of {1, 2, 3, 4} in graph (a), since in these two sortings all edges start from left to right, which satisfies the requirement of a topological sorting. The property of topological sorting of DAGs yields the following lemma.

Lemma 3. (Zheng et al., 2019) For a DAG with adjacency matrix $\mathcal{A} \in \mathbb{R}^{N \times N}$, there exists an orthogonal matrix $Q \in \mathbb{R}^{N \times N}$ such that $\bar{\mathcal{A}} = Q^{-1}\mathcal{A}Q$ is a lower-triangular matrix.

This study assumes no communication time delays. Interested readers are referred to di Bernardo et al. (2015), Zhang and Orosz (2016), Petrillo et al. (2018) for studies on communication time delays.

2.3. Control objective of multi-vehicle systems

Denote the desired inter-vehicle distance between two consecutive vehicles by a constant $d_0 \in \mathbb{R}^+$. Then the control objective of multi-vehicle systems becomes: $\forall\, i \in \mathcal{N}$,

$$\lim_{t \to +\infty} \|p_i(t) - p_{i-1}(t) + d_0\| = 0,$$
$$\lim_{t \to +\infty} \|v_i(t) - v_{i-1}(t)\| = 0,$$
$$\lim_{t \to +\infty} \|a_i(t) - a_{i-1}(t)\| = 0.$$

Denote the desired state offset between vehicles i and j by $\widetilde{d}_{ji} := [(j-i)\cdot d_0, 0, 0]^\top$, which satisfies:

$$A\widetilde{d}_{ji} = \widetilde{d}_{ji} = -\widetilde{d}_{ij}. \tag{3}$$

Then the control objective can be rewritten as: $\forall\, i, j \in \{0\} \cup \mathcal{N}$,

$$\lim_{t \to +\infty} \|x_i(t) - x_j(t) - \widetilde{d}_{ji}\| = 0. \tag{4}$$

Remark 1. Different from Wang et al. (2016), Bian et al. (2019) which use the constant time headway policy in control objective design, this study considers the constant spacing policy, as is done in Dunbar and Caveney (2012), Zheng et al. (2017), Gong et al. (2016). In this case, vehicles' velocity information is not involved in the desired headway, which brings less restrictions on communication topology design.

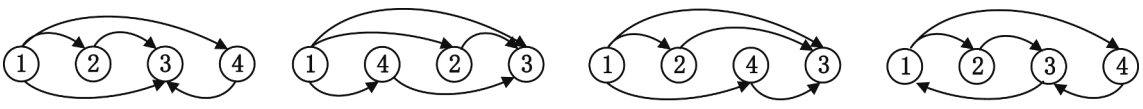

(a) Graph 1 (b) Graph 2 (c) Graph 3 (d) Graph 4

Fig. 1. Illustration of DAGs and topological sortings: (a)-(c) are DAGs, (d) is not a DAG.

3. Design of distributed model predictive controller

This section details the design of the proposed distributed model predictive controller. The open-loop optimization problem is formulated first, with which a DMPC algorithm is then designed.

3.1. Open-loop Optimization Problem

At time t, vehicle i can only use the information of its neighboring vehicles j, $j \in \mathbb{I}_i(t)$ for control input optimization. Denote by N_p the predictive horizon, then we define the following three types of state and control input trajectories within the predictive time horizon $[t, t+N_p]$:

1. $x_i^p(k|t)$, $k \in \{0\} \cup \mathbb{K}_1$ and $u_i^p(k|t)$, $k \in \mathbb{K}_0$: predicted state trajectory and control input trajectory;
2. $x_i^*(k|t)$, $k \in \{0\} \cup \mathbb{K}_1$ and $u_i^*(k|t)$, $k \in \mathbb{K}_0$: optimal state trajectory and control input trajectory;
3. $x_i^a(k|t)$, $k \in \{0\} \cup \mathbb{K}_1$ and $u_i^a(k|t)$, $k \in \mathbb{K}_0$: assumed state trajectory and control input trajectory.

Here the predicted trajectories parameterize the optimization problem, while the optimal trajectories represent the optimal solution to the optimization problem. The assumed trajectories are generated from the optimal trajectories through last-step shifting, and will be transmitted to out-neighbor vehicles $\mathbb{O}_i(t)$ (see step 4 in Algorithm 1). Now the open-loop optimization problem for vehicle i ($i \in \mathcal{N}$) at time $t \geqslant 0$ is formulated as follows:

Problem $\mathcal{P}_i(t)$:

$$\min_{u_i^p(k|t),k\in\mathbb{K}_0} J_i(x_i^p, u_i^p, x_i^a, x_{j\in\mathbb{I}_i(t)}^a;\mathbb{K}_0|t) = \sum_{k=0}^{N_p-1} l_i(x_i^p, u_i^p, x_i^a, x_{j\in\mathbb{I}_i(t)}^a;k|t) \tag{5a}$$

subject to:

$$x_i^p(0|t) = x_i(t), \tag{5b}$$

$$x_i^p(k+1|t) = Ax_i^p(k|t) + Bu_i^p(k|t),\ k \in \mathbb{K}_0, \tag{5c}$$

$$u_i^p(k|t) \in \mathcal{U}_i,\ k \in \mathbb{K}_0, \tag{5d}$$

$$x_i^p(N_p|t) = \frac{x_j^a(N_p|t) + \widetilde{d}_{ji}}{|\mathbb{I}_i(t)|}, \quad \text{if } |\mathbb{I}_i(t)| > 0, \tag{5e}$$

$$\gamma_i(t) \sum_{k=1}^{N_p-1} \|x_i^p(k|t) - x_i^a(k|t)\|_{G_i} \leqslant \sum_{k=1}^{N_p-1} \|x_i^p(k|t-1) - x_i^a(k|t-1)\|_{G_i}, \tag{5f}$$

where $\gamma_i(t) > 0$ is a *self-deviation constriction factor*, and $l_i(\cdot)$ in cost function (5a) has the following form:

$$l_i(x_i^p, u_i^p, x_i^a, x_{j\in\mathbb{I}_i(t)}^a;k|t) = \|u_i^p(k|t)\|_{R_i} + \|x_i^p(k|t) - x_i^a(k|t)\|_{F_i} + \sum_{j\in\mathbb{I}_i(t)} \|x_i^p(k|t) - x_j^a(k|t) - \widetilde{d}_{ji}\|_{G_i}, \tag{6}$$

where R_i, F_i, and G_i are vehicle i's positive definite weight matrices with proper dimensions.

In Problem $\mathcal{P}_i(t)$, the cost function (6) contains three terms: (1) the first term corresponds to the penalty on the control input with a weight matrix R_i; (2) the second term corresponds to the penalty on the deviation between vehicle i's predicted and assumed trajectories (or *self deviation* for short) with a weight matrix F_i; and (3) the third term corresponds to the penalty on the deviation between vehicle i's predicted trajectory and its neighbors' assumed trajectories with offset $\widetilde{d}_{ji}$ (or *neighbor deviation* for short) with a weight matrix G_i. Hereinafter, the second and third terms of (6) are called the *self-deviation penalty* and *neighbor-deviation penalty*, respectively, while F_i and G_i the *self-deviation weight* and *neighbor-deviation weight*, respectively.

In Problem $\mathcal{P}_i(t)$, constraints (5b), (5c), and (5d) represents the constraints from initial states, vehicle dynamics, and control inputs, respectively. Terminal equality constraint (5e), called the *neighbor-deviation constraint* and similar to the one proposed in Zheng et al. (2017), requires vehicle i's predictive terminal state to equal the average of its neighbors' assumed terminal states with offset $\widetilde{d}_{ij}$. Moreover, inequality constraint (5f), called the *self-deviation constraint*, requires vehicle i's weighted self deviation at time t to be contracted by a positive factor $\gamma_i(t)$ compared to that at time $t-1$.

Problem $\mathcal{P}_i(t)$ contains only vehicle i's and its current neighbors' information, so it is a distributed optimization problem.

Remark 2. In contrast to the optimization problem designed in Zheng et al. (2017) for fixed communication topologies, the main difference of Problem $\mathcal{P}_i(t)$ lies in the extra constraint (5f) for switching communication topologies. In detail, the greater the self-deviation constriction factor $\gamma_i(t)$ in (5f) is, the more the weighted self deviation is constricted. This helps mitigates the impact of topology switching on trajectory deviation. Together with constraint (5e), which will be used to facilitate the convergence analysis of predicted terminal states (see Theorem 1 in Section 4.A), constraint (5f) will be used to facilitate the stability analysis of the closed-loop system (see Theorem 2 in Section 4.B).

3.2. DMPC algorithm

With the proposed Problem $\mathcal{P}_i(t)$ above, a DMPC algorithm is designed accordingly. Based on the implementation and communication schemes, the existing DMPC algorithms can be divided into two categories: (1) parallel DMPC (Wang et al., 2016), where optimization problems are solved by multiple agents simultaneously; and (2) serial DMPC (Zhou et al., 2019), where optimization problems are solved by agents sequentially. Here we consider parallel DMPC, since it has better scalability than serial DMPC.

Assume that Problem $\mathcal{P}_i(t)$ can be solved in one control loop. Then, based on the designed open-loop optimization problem, the DMPC algorithm is designed in Algorithm 1. The operation of Algorithm 1 is further illustrated in Fig. 2. As Fig. 2 shows, the input of vehicle i's Problem $\mathcal{P}_i(t)$ includes the assumed state and control input trajectories of its own (*i.e.*, $x_i^a(k|t)$, $k \in \{0\} \cup \mathbb{K}_1$ and $u_i^a(k|t)$, $k \in \mathbb{K}_0$) and its neighbors (*i.e.*, $x_j^a(k|t)$, $k \in \{0\} \cup \mathbb{K}_1$ and $u_j^a(k|t)$, $k \in \mathbb{K}_0$, $j \in \mathbb{N}_i(t)$), while the output is vehicle i's optimal state and control input trajectories (*i.e.*, $x_i^*(k|t)$, $k \in \{0\} \cup \mathbb{K}_1$ and $u_i^*(k|t)$, $k \in \mathbb{K}_0$). The first optimal control input $u_i^*(0|t)$ is used for vehicle control, while the entire optimal trajectories at time t are used to generate the assumed trajectories at time $t+1$ through last-step shifting (*i.e.*, step 8 in Algorithm 1).

Algorithm 1. The DMPC Algorithm

At time $t = 0$: all vehicles $i \in \mathcal{N}$

1: Initialize $u_i^p(k|0)$ and $x_i^p(k|0)$:

$$u_i^p(k|0) = 0,\ k \in \mathbb{K}_0,$$
$$x_i^p(k|0) = \begin{cases} x_i(0), & k = 0, \\ Ax_i^p(k-1|0), & k \in \mathbb{K}_1. \end{cases}$$

2: Use $u_i^p(0|0)$ for vehicle control for time 0;

3: Calculate $u_i^a(k|1)$ and $x_i^a(k|1)$:

$$u_i^a(k|1) = \begin{cases} u_i^p(k+1|0), & k \in \mathbb{K}_0 \backslash \{N_p - 1\}, \\ 0, & k = N_p - 1, \end{cases}$$
$$x_i^a(k|1) = \begin{cases} x_i^p(k+1|0), & k \in \mathbb{K}_0, \\ Ax_i^p(N_p|0), & k = N_p. \end{cases}$$

At time $t \geqslant 1$: all vehicles $i \in \mathcal{N}$

4: Transmit $x_i^a(k|t)$, $k \in \{0\} \cup \mathbb{K}_1$ to out-neighbor vehicle $j \in \mathbb{O}_i(t)$ through communication;

5: Receive $x_j^a(k|t)$, $k \in \{0\} \cup \mathbb{K}_1$ from in-neighbor vehicle $j \in \mathbb{N}_i(t)$ through communication;

6: Solve Problem $\mathcal{P}_i(t)$ and obtain $u_i^*(k|t)$, $k \in \mathbb{K}_0$ and $x_i^*(k|t)$, $k \in \{0\} \cup \mathbb{K}_1$;

7: Use $u_i^*(0|t)$ for vehicle control for time t;

8: Calculate $u_i^a(k|t+1)$ and $x_i^a(k|t+1)$:

$$u_i^a(k|t+1) = \begin{cases} u_i^*(k+1|t), & k \in \mathbb{K}_0 \backslash \{N_p - 1\}, \\ \mathbb{O}, & k = N_p - 1, \end{cases}$$
$$x_i^a(k|t+1) = \begin{cases} x_i^*(k+1|t), & k \in \mathbb{K}_0, \\ Ax_i^*(N_p|t), & k = N_p. \end{cases}$$

Algorithm 1 contains only vehicle i's and its current neighbors' information, so it can be implemented is a distributed manner. Moreover, according to Algorithm 1, following vehicles solve optimization problems simultaneously in each control step, so it is a parallel DMPC algorithm.

4. Stability analysis for the closed-loop system

This section presents the stability analysis for the closed-loop system. The convergence of predicted terminal states is first analyzed, based on which the stability of the closed-loop system is then analyzed.

4.1. Convergence analysis of predicted terminal states

We first prove that vehicle i's predicted terminal state $x_i^*(N_p|t)$ will converge to vehicle 0's predicted terminal state $x_0(t+N_p)$ with offset $\widetilde{d}_{0i}$ under specific conditions.

Define the terminal state error as:

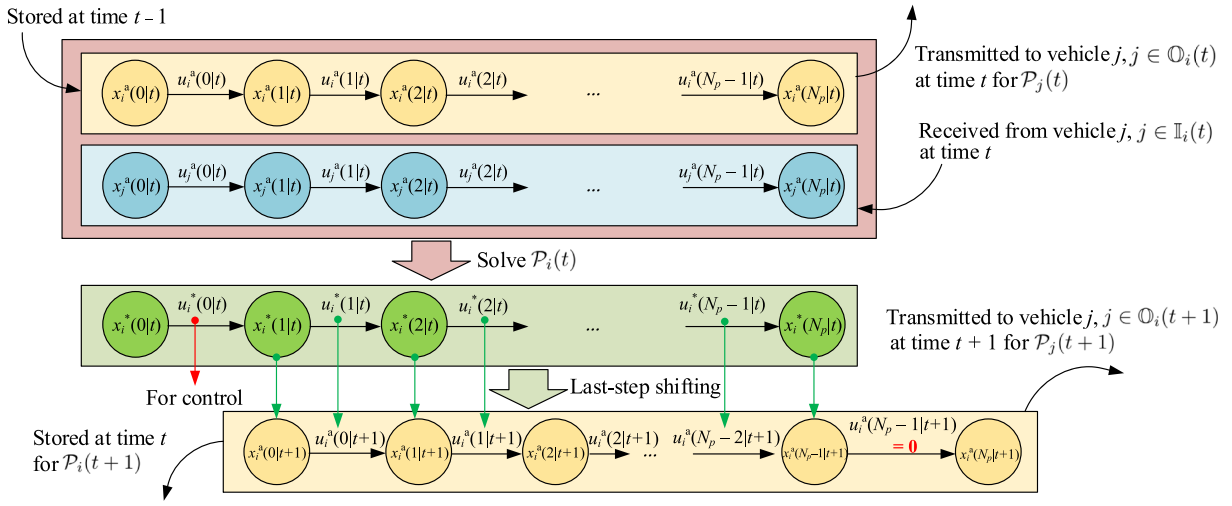

Fig. 2. Illustration of the DMPC algorithm ($t \geqslant 1$).

$$\widetilde{x}_i(N_p|t+1) = x_i^*(N_p|t+1) - x_0(t+1+N_p) + \widetilde{d}_{i0}.$$

When the leading vehicle runs at a constant velocity, we have:

$$x_0(t+k) = Ax_0(t+k-1).$$

Then, if $|\mathbb{I}_i(t+1)| > 0$, it holds that:

$$\begin{aligned}\widetilde{x}_i(N_p|t+1) &= \tfrac{1}{|\mathbb{I}_i(t+1)|}\textstyle\sum_{j\in\mathbb{I}_i(t+1)}(x_j^a(N_p|t+1) + \widetilde{d}_{ji}) - x_0(t+1+N_p) + \widetilde{d}_{i0}\\ &= \tfrac{1}{|\mathbb{I}_i(t+1)|}\textstyle\sum_{j\in\mathbb{I}_i(t+1)}(Ax_j^*(N_p|t) - Ax_0(t+N_p) + \widetilde{d}_{j0})\\ &= \tfrac{1}{|\mathbb{I}_i(t+1)|}A\textstyle\sum_{j\in\mathbb{I}_i(t+1)}(x_j^*(N_p|t) - x_0(t+N_p) + \widetilde{d}_{j0})\\ &= \tfrac{1}{|\mathbb{I}_i(t+1)|}A\textstyle\sum_{j\in\mathbb{I}_i(t+1)}\widetilde{x}_j(N_p|t),\end{aligned}$$

where the first three equalities use (5e), (2), and (3), respectively. Define the aggregated terminal state error as $\widetilde{X}(N_p|t+1) = [\widetilde{x}_1^\top(N_p|t+1), \widetilde{x}_2^\top(N_p|t+1), ..., \widetilde{x}_N^\top(N_p|t+1)]^\top$. If $|\mathbb{I}_i(t+1)| > 0, \forall\, i \in \mathcal{N}$ holds, we have:

$$\widetilde{X}(N_p|t+1) = (\Lambda(t+1)\mathcal{A}(t+1)) \otimes A\cdot\widetilde{X}(N_p|t), \tag{7}$$

where

$$\Lambda(t+1) \coloneqq \operatorname{diag}\left\{\frac{1}{|\mathbb{I}_1(t+1)|}, \frac{1}{|\mathbb{I}_2(t+1)|}, ..., \frac{1}{|\mathbb{I}_N(t+1)|}\right\}.$$

For the term $\Lambda(t+1)\mathcal{A}(t+1)$ in (7), we have the following lemma.

Lemma 4. *If communication topology $\mathcal{G}_i$ is a DAG with a spanning tree rooted at the leading vehicle, then $\Lambda_i\mathcal{A}_i$ is a nilpotent matrix, i.e., there exists a constant integer N_i satisfying $0 \leqslant N_i \leqslant N$ such that $(\Lambda_i\mathcal{A}_i)^{N_i} = 0$.*

Proof. Since $\mathcal{G}_i$ is a DAG, according to Lemma 3, there exists an orthogonal matrix Q_i such that $\bar{\mathcal{A}}_i = Q_i^{-1}\mathcal{A}_iQ_i$ is lower-triangular. Since $\mathcal{G}_i$ contains no self-loops, the diagonal elements of $\bar{\mathcal{A}}_i$ are 0, so $\bar{\mathcal{A}}_i$ is a nilpotent matrix. Denote by $N_i \in \mathbb{N}^+$ the index of $\bar{\mathcal{A}}_i$, *i.e.*, $\bar{\mathcal{A}}_i^{N_i} = 0$, then we know $0 \leqslant N_i \leqslant N$. Moreover, since Λ_i is a diagonal matrix, we know $\bar{\Lambda}_i = Q_i^{-1}\Lambda_iQ_i$ is also a diagonal matrix. Therefore, $\bar{\mathcal{A}}_i\bar{\Lambda}_i$ is also a nilpotent matrix, and its index is less than or equal to N_i, so we have $(\bar{\mathcal{A}}_i\bar{\Lambda}_i)^{N_i} = 0$. Then we have:

$$(\Lambda_i\mathcal{A}_i)^{N_i} = (\Lambda_iQ_i\bar{\mathcal{A}}_iQ_i^{-1})^{N_i} = \Lambda_iQ_i(\bar{\mathcal{A}}_i\bar{\Lambda}_i)^{N_i-1}\bar{\mathcal{A}}_iQ_i^{-1} = \Lambda_iQ_i(\bar{\mathcal{A}}_i\bar{\Lambda}_i)^{N_i}(\Lambda_iQ_i)^{-1} = 0.$$

Based on Lemma 4, we have the following theorem on the convergence of predicted terminal state errors. □

Theorem 1. When the leading vehicle runs at a constant velocity, if there exists a DAG $\mathcal{G}_i \in \mathbb{G}$ with a spanning tree rooted at the leading vehicle, and a time period $[t_1, t_1+N_i-1]$ such that $\mathcal{G}(t) \equiv \mathcal{G}_i, \forall\, t \in \{t_1, t_1+1, t_1+2, ..., t_1+N_i-1\}$, then the predicted terminal state errors converge to 0 at $t = t_1+N_i-1$, *i.e.*,

$$\widetilde{X}(N_p|t_1+N_i-1) = 0.$$

Proof. Since $\mathcal{G}_i$ is a DAG with a spanning tree rooted at the leading vehicle, we know that $|\mathbb{I}_i(t)| > 0, \forall\, i \in \mathcal{N}$ and $\forall\, t \in \{t_1, t_1+1, t_1+2, ..., t_1+N_i-1\}$. Then we have:

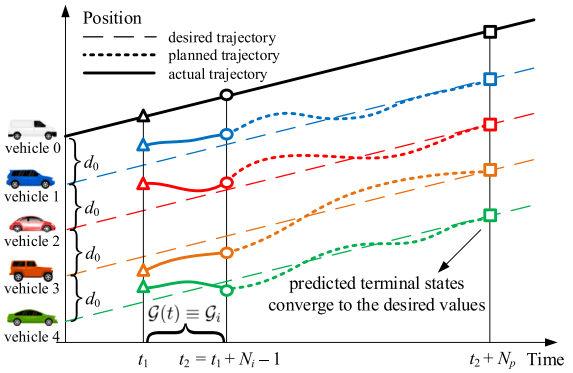

Fig. 3. Convergence of predicted terminal states.

$$\begin{aligned}\widetilde{X}(N_p|t_1+N_i-1) &= \left(\prod_{k=t_1}^{t_1+N_i-1}(\Lambda(k)\mathcal{A}(k)\otimes A)\right)\cdot\widetilde{X}(N_p|t_1-1)\\ &= \left(\prod_{k=t_1}^{t_1+N_i-1}(\Lambda(k)\mathcal{A}(k))\otimes A^{N_i}\right)\cdot\widetilde{X}(N_p|t_1-1)\\ &= ((\Lambda_i\mathcal{A}_i)^{N_i}\otimes A^{N_i})\cdot\widetilde{X}(N_p|t_1-1)\\ &= 0,\end{aligned}$$

where the first and last equalities use (7) and Lemma 4, respectively.

Theorem 1 requires the communication topology to be fixed for a short time period so that the predicted terminal state errors converge to zero, as shown in Fig. 3. This requirement is acceptable in practice considering that this time period is no longer than N control steps, *i.e.*, the number of following vehicles in the multi-vehicle system. Moreover, note that if the leading vehicle keeps moving at a constant velocity, the communication topology does not need to be fixed after the convergence, and its switching does not affect the convergence any more. This is because the following vehicles use 0 as their last assumed control inputs in the the following optimization calculation, as presented in Algorithm 1, so their predicted terminal states evolute with the constant velocity as the leading vehicle no matter the communication topology switches or not, which guarantees the convergence. □

Remark 3. Compared with Zheng et al. (2017), which also provides a theorem for the convergence of predicted terminal states but requires unidirectional communication topologies (a specific class of DAG-type topologies), Theorem 1 is suitable for DAG-type communication topologies. This enlarges the application range of this theorem in terms of feasible communication topologies.

Remark 4. Theorem 1, as well as Theorem 2 given below, requires the leading vehicle to move at a constant velocity, as is considered in Zheng et al. (2017), Dunbar and Caveney (2012). This requirement is reasonable in practice since platoons are mainly running at a relative constant velocity most of the time. In this case, the state and acceleration of the leading vehicle can be viewed as the equilibrium point and disturbance of the platoon respectively for stability analysis. We also refer interested readers to some recent studies, *e.g.*, Gong et al. (2016), Yu et al. (2018), that have the potential to deal with the case of a dynamic leader.

4.2. Stability analysis of the closed-loop system

When the predicted terminal states converge to their desired values, as stated in Theorem 1, the convergence of tracking errors is guaranteed with the following theorem.

Theorem 2. When the leading vehicle runs at a constant velocity, and the predicted terminal state errors converge to 0, if there exists a time constant $t_0 \geqslant 0$ such that Problem $\mathcal{P}_i(t_0)$ is feasible, then the closed-loop system is asymptotically stable if the following condition is satisfied:

$$F_i \geqslant (|\mathbb{B}_i|+1)\left(\left(\frac{|\mathbb{A}_i \backslash \mathbb{I}_i(t)|}{\gamma_i(t)}\right)^2 \cdot G_i + \sum_{j\in\mathbb{B}_i} G_j\right),\ \forall\, t \geqslant t_0. \tag{8}$$

Proof. See Appendix. □

Remark 5. The proof of Theorem 2 is based on a CLF $V_{\mathbb{A}} = \sum_{i=1}^{N} V_{\mathbb{A}_i}$ defined on the joint neighbor set $\mathbb{A}_i$, rather than the commonly used Lyapunov function $V_{\mathbb{I}} = \sum_{i=1}^{N} V_{\mathbb{I}_i(t)}$ defined on the current neighbor set $\mathbb{I}_i(t)$ (see Dunbar and Caveney (2012, 2017)). Actually, $V_{\mathbb{I}}$ is always upperbounded by $V_{\mathbb{A}}$, *i.e.*, $V_{\mathbb{I}} \leqslant V_{\mathbb{A}}$, $\forall\, t \geqslant 0$. Therefore, though $V_{\mathbb{I}}$ may either increase or decrease due to the switching of communication topologies, its upperbound $V_{\mathbb{A}}$ is designed to be monotonically decreasing (see Fig. 4), thus can serve as a CLF for the switching system.

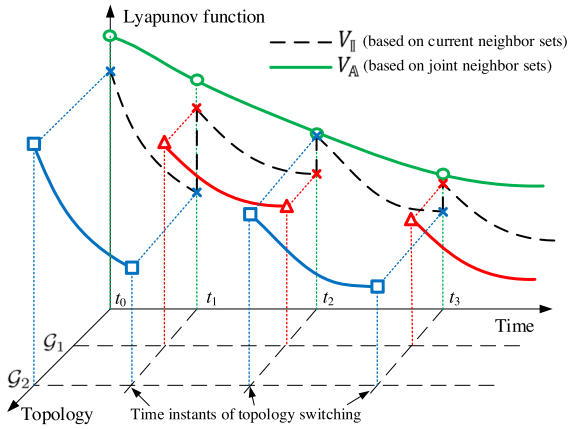

Fig. 4. The joint-neighbor-set based CLF.

Remark 6. Theorem 2 requires Problem $\mathcal{P}_i(t)$ to be initially feasible at $t = t_0$ for all $i \in \mathcal{N}$. The requirement is widely used in the literature, *e.g.*, Dunbar and Caveney (2012), Zheng et al. (2017). Given initial feasibility, Problem $\mathcal{P}_i(t)$ is recursively feasible even thought the communication topology switches. In detail, when the leading vehicle moves at a constant velocity and the terminal state error converges to 0, it is not difficult to check that $[u^*(1|t), u^*(2|t), u^*(3|t), ..., u^*(N_p - 1|t), 0]$ satisfies all the constraints in Problem $\mathcal{P}_i(t+1)$ even when the communication topology switches, where $[u^*(0|t), u^*(1|t), u^*(2|t), ..., u^*(N_p - 2|t), u^*(N_p - 1|t)]$ is vehicle i's optimal solution to Problem $\mathcal{P}_i(t)$. This method, presented in the Proof of Theorem 2, is also widely used in the literature, *e.g.*, Dunbar and Caveney (2012), Zheng et al. (2017). Specifically, in the case that initial feasibility is not guaranteed, since control input set constraint (5d) may be too restrictive to satisfy terminal constraint (5e), one possible solution is to increase the predictive horizon N_p, so that vehicles have enough time to adjust their terminal states.

Remark 7. According to (8), the lower bound of a vehicle's self-deviation weight F_i has a positive relationship with the summation of the vehicle's out-neighbors' neighboring-deviation weights $\sum_{j\in\mathbb{B}_i} G_j$, as well as the number of the out-neighbors $|\mathbb{B}_i|$. This result is partially consistent with that of Zheng et al. (2017). In contrast to the stability condition in Zheng et al. (2017), (8) has an extra term of $\left(\frac{|\mathbb{A}_i \setminus \mathbb{I}_i(t)|}{\gamma_i(t)}\right)^2 \cdot G_i$ in the lower bound of F_i. According to this term, given $\sum_{j\in\mathbb{B}_i} G_j$ and G_i, when the number of failed communication channels $|\mathbb{A}_i \setminus \mathbb{I}_i(t)|$ increases, we can increase either vehicle i's self-deviation weight F_i, or its self-deviation constriction factor $\gamma_i(t)$, to maintain system stability. This reflects the complementary functions of cost function adjustment (by increasing the self-deviation penalty) and constraint adjustment (by enhancing the self-deviation constriction) in addressing communication topology switching.

According to Remark 7, in order to use a constant F_i for better control performance, $\gamma_i(t)$ can be set as:

$$\gamma_i(t) = \sqrt{c} \cdot |\mathbb{A}_i \setminus \mathbb{I}_i(t)| + \delta_i, \tag{9}$$

where $c > 0$ is a constant and δ_i equals 0 when $|\mathbb{A}_i \setminus \mathbb{I}_i(t)| > 0$, or takes an arbitrary positive value when $|\mathbb{A}_i \setminus \mathbb{I}_i(t)| = 0$. Then we have the following corollary.

Corollary 1. Suppose that $\gamma_i(t)$ in Problem $\mathcal{P}_i(t)$ is selected according to (9). When the leading vehicle runs at a constant velocity, and the predicted terminal state errors converge to 0, if there exists a time constant $t_0 \geqslant 0$ such that Problem $\mathcal{P}_i(t_0)$ is feasible, then the closed-loop system is asymptotically stable if the following condition is satisfied:

$$F_i \geqslant (|\mathbb{B}_i| + 1)\left(\frac{G_i}{c} + \sum_{j\in\mathbb{B}_i} G_j\right), \forall\, t \geqslant t_0. \tag{10}$$

Considering that a large γ_i may cause constraint (5f) to be restrictive, a small δ_i is recommended when $|\mathbb{A}_i \setminus \mathbb{I}_i(t)| = 0$, while c can be selected to balance the feasibility range of constraint (5f) and the restriction on F_i in (10). Note that constraint (5f) is always feasible, since $x_i^p(k|t) = x_i^a(k|t)$, $k = 1, 2, ..,N_p - 1$ always satisfies constraint (5f).

In particular, if the communication topology is fixed without any switching, it holds that $|\mathbb{A}_i \setminus \mathbb{I}_i(t)| = 0, \forall\, t \geqslant 0$. In this case, constraint (5f) in Problem $\mathcal{P}_i(t)$ can be removed. Then we have the following corollary, which is fully consistent with the result of Zheng et al. (2017).

Corollary 2. Suppose that the communication topology is fixed and constraint (5f) in Problem $\mathcal{P}_i(t)$ is removed. When the leading vehicle runs at a constant velocity, and the predicted terminal state errors converge to 0, if there exists a time constant $t_0 \geqslant 0$ such that Problem $\mathcal{P}_i(t_0)$ is feasible, then the closed-loop system is asymptotically stable if the following condition is satisfied:

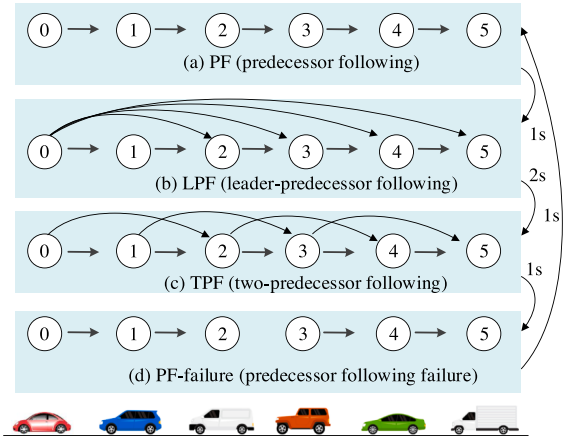

Fig. 5. Switching communication topologies used in numerical simulations.

$$F_i \geqslant |\mathbb{B}_i| \sum_{j\in\mathbb{B}_i} G_j,\ \forall\ t \geqslant t_0.$$

5. Numerical Simulation

This section presents numerical simulations to demonstrate the correctness of the proposed theorems.

In numerical simulations, we consider a vehicle platoon consisting of 1 leading vehicle and $N = 5$ following vehicles. Four types of possible communication topologies are considered, *i.e.*, PF, LPF, TPF, and PF-failure, as shown in Fig. 5. Note that in the PF-failure topology, the communication channel between vehicles 2 and 3 is broken, which will cause the instability of the system.

In controller design, the predictive horizon is $N_p = 20$, and the desired inter-vehicle distance is $d_0 = 20$ [m]. The initial position of the leading vehicle is $p_0(0) = 0$ [m], while the initial states of the following vehicles are $p_i(0) = -i{\cdot}d_0 + d_e$ [m], $v_i(0) = 10 + v_e$ [m/s], and $a_i(0) = 0$ [m/s^2], where d_e and v_e are initial position and velocity errors. The simulation parameters and model/controller parameters are listed in Table 1.

Considering different communication topology conditions, leading vehicle behaviors, and vehicle model conditions, we conduct the following four sets of numerical simulations.

5.1. Case I: fixed communication topologies and a static leader

First, we consider the case of fixed communication topologies and a static leader. In this case, the leading vehicle runs at a constant velocity $v_0(t) = 10$ [m/s], while the communication topology remains fixed. Simulation results corresponding to the 4 types of communication topologies are shown in Fig. 6.

As Fig. 6 shows, for the PF, LPF, and TPF topologies, the position and velocity errors of all the following vehicles converge to zero

Table 1
Vehicle model parameters.

parameter ($i \in \mathcal{N}$)	unit	value
Δt	s	0.1
N	–	5
m_i	kg	$1500 + 400 \times i$
r_i	m	$0.25 + 0.06 \times i$
η_i	–	$0.80 + 0.08 \times i$
τ_i	s	$0.4 + 0.02 \times i$
$C_{A,i}$	kg/m	$0.40 + 0.10 \times i$
f_i	-	$0.015 + 0.006 \times i$
g	N/kg	9.80
$\mathcal{U}_i$	m/s^2	$[-3, 3]$
R_i	–	0.1
G_i	–	diag{5, 2.5, 1}
F_i	–	$(|\mathbb{B}_i| + 1)^2{\cdot}G_i$
$\gamma_i(t)$	–	$|\mathbb{A}_i \backslash \mathbb{I}_i(t)| + \delta_i$

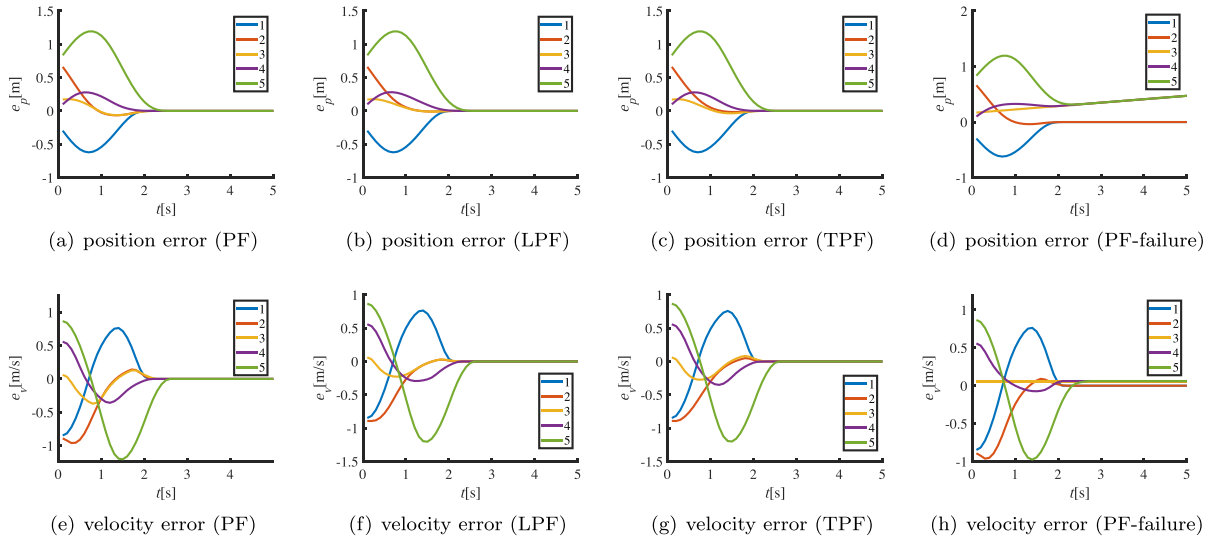

Fig. 6. Simulation results in Case I.

asymptotically, while the PF-failure topology causes the instability of the platoon, since the position and velocity errors of vehicles 3, 4, and 5 cannot converge to zero. This is because there does not exist a directed spanning tree rooted at the leading vehicle in the PF-failure topology.

5.2. Case II: switching communication topologies and a static leader

Next, we consider the case of switching communication topologies and a static leader. In this case, the leading vehicle runs at a constant velocity $v_0(t) = 10$ [m/s], while the communication topologies switch among the 4 types of communication topologies. In detail, as shown in Fig. 5, the initial communication topology is PF, and it switches to LPF after 1 s, to TPF after another 2 s, to PF-failure after another 1 s, and so on so forth. Simulation results are shown in Fig. 7.

As Fig. 7 shows, the position and velocity errors of all the following vehicles converge to zero asymptotically. This means the platoon is asymptotically stable even in the present of the PF-failure topology. Moreover, the control input constraint is satisfied for all the following vehicles. This demonstrates the effectiveness of Theorem 2 for a static leader.

5.3. Case III: switching communication topologies and a dynamic leader

Then, we consider a dynamic leader with a sinusoidal acceleration. In this case, the leading vehicle's initial velocity is $v_0(0) = 10$ [m/s], and its acceleration profile is given by:

$$a_0(t) = \begin{cases} 0, & 0\ \text{s} \leqslant t < 2\ \text{s}, \\ \sin(\pi(t-1)), & 2\ \text{s} \leqslant t < 6\ \text{s}, \\ 0, & t \geqslant 6\ \text{s}. \end{cases} \quad [\text{m/s}^2]$$

Moreover, this acceleration profile is *a priori known by the leading vehicle, and will be used by the leading vehicle to generate its assumed trajectory. Simulation results are shown in Fig. 8.*

As Fig. 8 shows, the position and velocity errors of all the following vehicles also converge to zero asymptotically when the leading vehicle finishes its acceleration. This means the platoon is asymptotically stable even in the present of the PF-failure topology. Moreover, the control input constraint is also satisfied for all the following vehicles. This demonstrates the effectiveness of Theorem 2 for a dynamic leader.

In particular, from the velocity profiles in Fig. 8(c), it is observed that the following vehicles start to accelerate or decelerate even before the action of the leading vehicle. This is attributed to the sharing of assumed trajectories in the control algorithm that helps the following vehicles better predict predecessors' behaviors. This phenomenon demonstrates the advantage of the DMPC controller in terms of far-sighted control optimization. Moreover, it is observed that string stability is not guaranteed even thought the platoon is asymptotically stable. We refer interested readers to Dunbar and Caveney (2012), Zhou et al. (2019), which have the potential to address string stability under the DMPC framework by directly incorporating spacing constraints or properly tuning weight matrices in the design of optimization problems.

5.4. Case IV: model mismatches and external disturbances

In this subsection, we consider the impact of model mismatches and external disturbances. In this case, all the following vehicles use a nominal time lag $\hat{\tau} = 0.46$ [s] to predict their own and neighbors' trajectories, which will cause model mismatches in trajectory

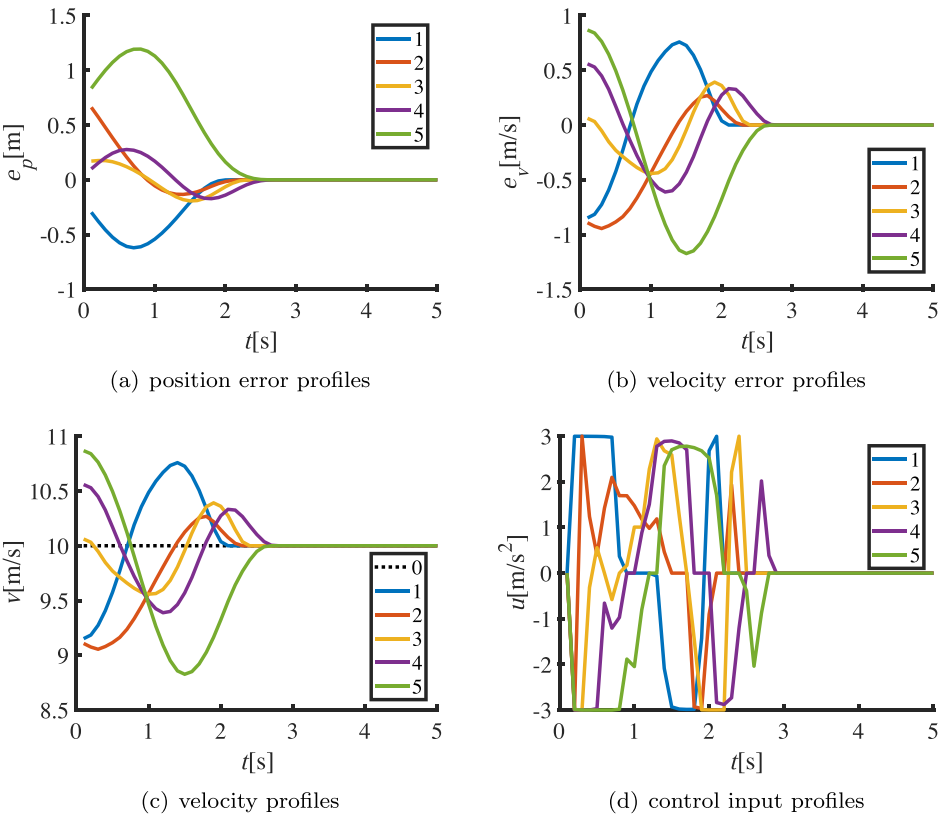

(a) position error profiles (b) velocity error profiles

(c) velocity profiles (d) control input profiles

Fig. 7. Simulation results in Case II.

prediction. Moreover, all the following vehicles also suffer from random control input disturbances $u_d \in [-0.1, 0.1]$ [m/s^2]. The other simulation conditions are the same as those of Case III. Simulation results are shown in Fig. 9.

As Fig. 9 shows, the position and velocity errors of all the following vehicles cannot strictly converge to zero when the leading vehicle finishes its acceleration. However, the tracking errors are minor and acceptable for platoon control. This demonstrates the robustness of the proposed controller to model mismatches and external disturbances.

5.5. Case V: performance comparison with centralized MPC

Finally, to demonstrate the optimality of the proposed DMPC controller, a numerical simulation study is carried out to compare it with a centralized MPC (CMPC) controller. The CMPC controller aggregates the cost functions and constraints in Problem $\mathcal{P}_i(t)$ for all $i \in \mathcal{N}$ but replaces $x_j^a(\cdot|t)$ with $x_j^p(\cdot|t)$ in cost function (5a) and constraint (5e). Constraint (5f) designed for DMPC is also removed. Simulation conditions in Case III are considered, while the following performance index is used for comparison.

$$J_r(t) := \sum_{i=1}^{N} \left(\|u_i(t)\|_{R_i} + \|x_i(t) - x_i^a(t)\|_{F_i} + \sum_{j \in \mathbb{I}_i(t)} \|x_i(t) - x_j(t) - \widetilde{d}_{ji}\|_{G_i} \right).$$

As Fig. 10 shows, both of the performance indices of the CMPC and DMPC controllers converge to zero, which demonstrates the asymptotic stability of the platoon. Moreover, the CMPC controller outperforms the DMPC controller with lower $J_r(t)$. This is attributed to the availability of global information in CMPC, *i.e.*, vehicles' realtime predicted trajectories $x_j^p(\cdot|t)$ instead of outdated assumed trajectories $x_j^a(\cdot|t)$ are used in the centralized optimization to avoid local optimum. In the meantime, the removal of constraint (5f) also expands the solution space and brings better performance. In particular, the accumulated performance indices $J_R := \sum_{t=0}^{15} J_r(t)$ of the CMPC and DMPC controllers are 302.81 and 377.00, respectively. This demonstrates that the DMPC controller reduces the performance by 24.50% compared with the CMPC controller, which, however, is acceptable considering that DMPC has lower communication requirements and better scalability.

6. Conclusion

This study proposed a DMPC method for the cooperation of multi-vehicle systems subject to switching communication topologies. In the DMPC algorithm, an open-loop optimization problem was formulated to incorporate neighbor-deviation and self-deviation

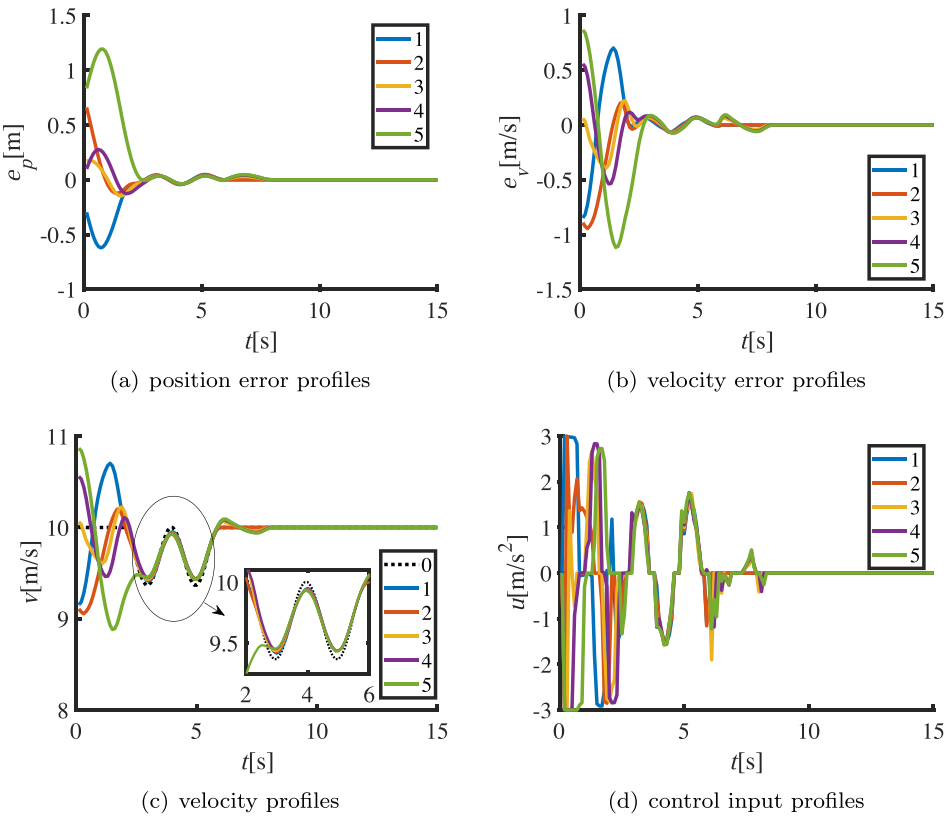

Fig. 8. Simulation results in Case III.

penalties and constraints. The neighbor-deviation constraint was used to derive a sufficient condition for the convergence of predicted terminal states (see Theorem 1) under DAG-type communication topologies, while the self-deviation constraint was used to ensure closed-loop system stability under switching communication topologies. Through Lyapunov analysis with a joint-neighbor-set based CLF, a sufficient condition on the weight matrices of the open-loop optimization problem was derived to guarantee the asymptotic stability of multi-vehicle systems subject to switching communication topologies (see Theorem 2).

In the future work, the robustness of the DMPC method will be studied to account for model uncertainties and external disturbances. String stability as well as time delays in communication channels and online computation also deserve further consideration.

Acknowledgment

This work was supported by the National Key R&D Program of China [Grant No. 2016YFB0100906]. Dr. Xu's work was supported by Key R&D Program of Hunan Province, China with 2019GK2151. The authors would like to thank Dr. Mengqi Xue from East China University of Science and Technology, Shanghai for his helpful suggestions to improve this work.

Appendix A. Proof of Theorem 2

Denote the optimal cost function at time $t \geqslant t_0$ by $J_i^*(t)$, *i.e.*,

$$J_i^*(t) = J_i(x_i^*, u_i^*, x_i^a, x_{j\in\mathbb{I}_i(t)}^a; \mathbb{K}_0|t) = \sum_{k=0}^{N_p-1} l_i(x_i^*, u_i^*, x_i^a, x_{j\in\mathbb{I}_i(t)}^a; k|t).$$

Then we have

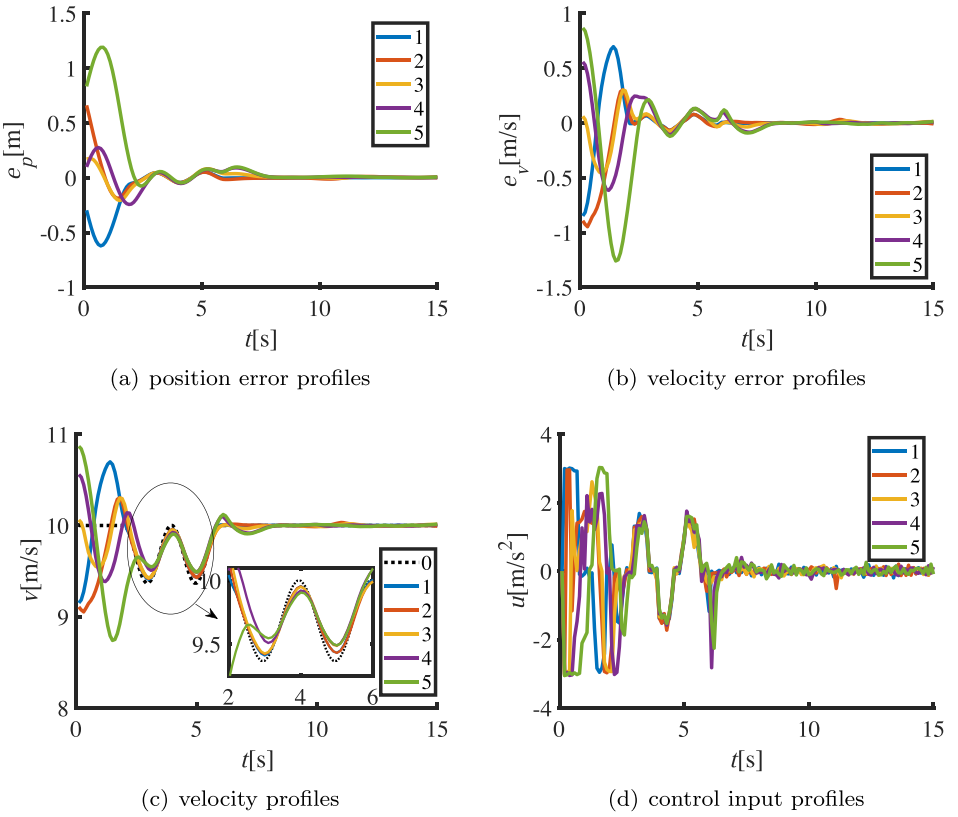

(a) position error profiles (b) velocity error profiles

(c) velocity profiles (d) control input profiles

Fig. 9. Simulation results in Case IV.

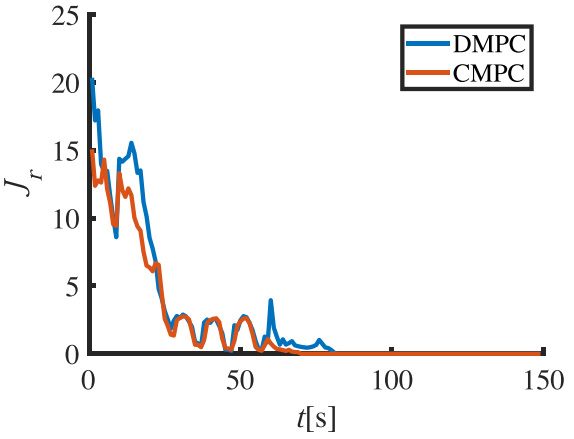

Fig. 10. Simulation results in Case V.

$$
\begin{aligned}
J_i^*(t+1) &= \sum_{k=0}^{N_p-1} l_i(x_i^*, u_i^*, x_i^a, x^a_{j\in\mathbb{I}_i(t+1)}; k|t+1) \\
&\leqslant \sum_{k=0}^{N_p-1} l_i(x_i^*, u_i^*, x_i^*, x^*_{j\in\mathbb{I}_i(t+1)}; k+1|t) \\
&= J_i(x_i^*, u_i^*, x_i^*, x^*_{j\in\mathbb{I}_i(t+1)}; \mathbb{K}_1|t),
\end{aligned} \tag{A.1}
$$

where the inequality uses the assumed trajectory in Algorithm 1, *i.e.*, $x_j^a(k|t+1) = x_j^*(k+1|t)$, as well as the optimality of J_i^* with respect to $x_i^*(k+1|t)$ and $u_i^*(k+1|t)$, *i.e.*, the following control input and state trajectories are a set of feasible solution to Problem $\mathcal{P}_i(t+1)$:

$$u_i^p(k|t+1) = u_i^*(k+1|t),\ k \in \mathbb{K}_0,$$
$$x_i^p(k|t+1) = x_i^*(k+1|t),\ k \in \mathbb{K}_0,$$

where $u_i^*(N_p|t) \coloneqq 0$ does not exist at time t but is defined here for notation convenience.

Consider the following Lyapunov function candidate:

$$V_{\mathbb{A}}(t) = \sum_{i=1}^{N} V_{\mathbb{A}_i}(t),$$

where

$$V_{\mathbb{A}_i}(t) = \sum_{k=0}^{N_p-1} l_i(x_i^*, u_i^*, x_i^a, x_{j\in\mathbb{A}_i}^a; k|t).$$

It is obvious that $V_{\mathbb{A}}(t) \geqslant 0$ for any $t \geqslant 0$, and $V_{\mathbb{A}}(t) = 0$ holds if and only if all the vehicles achieve their desired states.

According to (6), we have:

$$V_{\mathbb{A}_i}(t) = J_i^*(t) + \sum_{k=0}^{N_p-1} \sum_{j\in\mathbb{A}_i\setminus\mathbb{I}_i(t)} \|x_i^*(k|t) - x_j^a(k|t) - \widetilde{d}_{ji}\|.$$

Then it holds that:

$$\begin{aligned}
V_{\mathbb{A}_i}(t+1) &= J_i^*(t+1) + \sum_{k=0}^{N_p-1} \sum_{j\in\mathbb{A}_i\setminus\mathbb{I}_i(t+1)} \|x_i^*(k|t+1) - x_j^a(k|t+1) - \widetilde{d}_{ji}\|_{G_i} \\
&\leqslant J_i(x_i^*, u_i^*, x_i^*, x_{j\in\mathbb{I}_i(t+1)}^*; \mathbb{K}_1|t) + \sum_{k=0}^{N_p-1} \sum_{j\in\mathbb{A}_i\setminus\mathbb{I}_i(t+1)} \|x_i^*(k|t+1) - x_j^a(k|t+1) - \widetilde{d}_{ji}\|_{G_i} \\
&= J_i(x_i^*, u_i^*, x_i^*, x_{j\in\mathbb{A}_i}^*; \mathbb{K}_1|t) - \sum_{k=0}^{N_p-1} \sum_{j\in\mathbb{A}_i\setminus\mathbb{I}_i(t+1)} \|x_i^*(k+1|t) - x_j^a(k+1|t) - \widetilde{d}_{ji}\|_{G_i} \\
&\quad + \sum_{k=0}^{N_p-1} \sum_{j\in\mathbb{A}_i\setminus\mathbb{I}_i(t+1)} \|x_i^*(k|t+1) - x_j^a(k|t+1) - \widetilde{d}_{ji}\|_{G_i} \\
&\leqslant J_i(x_i^*, u_i^*, x_i^*, x_{j\in\mathbb{A}_i}^*; \mathbb{K}_1|t) + \sum_{k=0}^{N_p-1} \sum_{j\in\mathbb{A}_i\setminus\mathbb{I}_i(t+1)} \|x_i^*(k|t+1) - x_i^*(k+1|t)\|_{G_i} \\
&= J_i(x_i^*, u_i^*, x_i^*, x_{j\in\mathbb{A}_i}^*; \mathbb{K}_1|t) + |\mathbb{A}_i\setminus\mathbb{I}_i(t+1)| \sum_{k=1}^{N_p-1} \|x_i^*(k|t+1) - x_i^a(k|t+1)\|_{G_i},
\end{aligned}$$

where the first and second inequalities use (A.1) and Lemma 1, respectively.

Next, we analyze the increment of $V_{\mathbb{A}_i}$ at $t+1$:

$$\begin{aligned}
V_{\mathbb{A}_i}(t+1) - V_{\mathbb{A}_i}(t) \leqslant\ & J_i(x_i^*, u_i^*, x_i^*, x_{j\in\mathbb{A}_i}^*; \mathbb{K}_1|t) - J_i(x_i^*, u_i^*, x_i^a, x_{j\in\mathbb{A}_i}^a; \mathbb{K}_0|t) \\
& + |\mathbb{A}_i\setminus\mathbb{I}_i(t+1)| \sum_{k=1}^{N_p-1} \|x_i^*(k|t+1) - x_i^a(k|t+1)\|_{G_i},
\end{aligned} \tag{A.2}$$

For the first two terms in (A.2), we have:

$$\begin{aligned}
& J_i(x_i^*, u_i^*, x_i^*, x_{j\in\mathbb{A}_i}^*; \mathbb{K}_1|t) - J_i(x_i^*, u_i^*, x_i^a, x_{j\in\mathbb{A}_i}^a; \mathbb{K}_0|t) \\
=\ & \sum_{k=0}^{N_p-1} l_i(x_i^*, u_i^*, x_i^*, x_{j\in\mathbb{A}_i}^*; k+1|t) - \sum_{k=0}^{N_p-1} l_i(x_i^*, u_i^*, x_i^a, x_{j\in\mathbb{A}_i}^a; k|t) \\
=\ & \sum_{k=1}^{N_p-1} (l_i(x_i^*, u_i^*, x_i^*, x_{j\in\mathbb{A}_i}^*; k|t) - l_i(x_i^*, u_i^*, x_i^a, x_{j\in\mathbb{A}_i}^a; k|t)) + l_i(x_i^*, u_i^*, x_i^*, x_{j\in\mathbb{A}_i}^*; N_p|t) - l_i(x_i^*, u_i^*, x_i^a, x_{j\in\mathbb{A}_i}^a; 0|t) \\
=\ & \sum_{k=1}^{N_p-1} \left(-\|x_i^*(k|t) - x_i^a(k|t)\|_{F_i} + \sum_{j\in\mathbb{A}_i} \|x_i^*(k|t) - x_j^*(k|t) - \widetilde{d}_{ji}\|_{G_i} - \sum_{j\in\mathbb{A}_i} \|x_i^*(k|t) - x_j^a(k|t) - \widetilde{d}_{ji}\|_{G_i} \right) \\
& - l_i(x_i^*, u_i^*, x_i^a, x_{j\in\mathbb{A}_i}^a; 0|t) \\
\leqslant\ & - l_i(x_i^*, u_i^*, x_i^a, x_{j\in\mathbb{A}_i}^a; 0|t) + \sum_{k=1}^{N_p-1} \left(-\|x_i^*(k|t) - x_i^a(k|t)\|_{F_i} + \sum_{j\in\mathbb{A}_i} \|x_j^*(k|t) - x_j^a(k|t)\|_{G_i} \right),
\end{aligned} \tag{A.3}$$

where the third equality uses the condition of the convergence of predicted terminal states, *i.e.*,

$$l_i(x_i^*, u_i^*, x_i^*, x_{j\in\mathbb{A}_i}^*;N_p|t) = \|u_i^*(N_p|t)\|_{R_i} + \|x_i^*(N_p|t) - x_i^*(N_p|t)\|_{F_i} + \sum_{j\in\mathbb{A}_i} \|x_i^*(N_p|t) - x_j^*(N_p|t) - \widetilde{d}_{ji}\|_{G_i} = 0,$$

and the last inequality uses Lemma 1.

By substituting (A.3) into (A.2), we have:

$$\begin{aligned} &V_{\mathbb{A}_i}(t+1) - V_{\mathbb{A}_i}(t) \\ \leqslant &\sum_{k=1}^{N_p-1} \left(-\|x_i^*(k|t) - x_i^a(k|t)\|_{F_i} + \sum_{j\in\mathbb{A}_i} \|x_j^*(k|t) - x_j^a(k|t)\|_{G_i} + |\mathbb{A}_i \backslash \mathbb{I}_i(t+1)| \cdot \|x_i^*(k|t+1) - x_i^a(k|t+1)\|_{G_i} \right) \\ &- l_i(x_i^*, u_i^*, x_i^a, x_{j\in\mathbb{A}_i}^a;0|t). \end{aligned} \tag{A.4}$$

Consequently, we have:

$$\begin{aligned} &V_{\mathbb{A}}(t+1) - V_{\mathbb{A}}(t) \\ &= \sum_{i=1}^{N} (V_{\mathbb{A}_i}(t+1) - V_{\mathbb{A}_i}(t)) \\ &\leqslant -\sum_{i=1}^{N} l_i(x_i^*, u_i^*, x_i^a, x_{j\in\mathbb{A}_i}^a;0|t) + \sum_{i=1}^{N}\sum_{k=1}^{N_p-1} \left(-\|x_i^*(k|t) - x_i^a(k|t)\|_{F_i} + \sum_{j\in\mathbb{A}_i} \|x_j^*(k|t) - x_j^a(k|t)\|_{G_i} \right. \\ &\qquad \left. + |\mathbb{A}_i \backslash \mathbb{I}_i(t+1)| \cdot \|x_i^*(k|t+1) - x_i^a(k|t+1)\|_{G_i} \right) \\ &= -\sum_{i=1}^{N} l_i(x_i^*, u_i^*, x_i^a, x_{j\in\mathbb{A}_i}^a;0|t) + \sum_{i=1}^{N}\sum_{k=1}^{N_p-1} \left(-\|x_i^*(k|t) - x_i^a(k|t)\|_{F_i} + \sum_{j\in\mathbb{B}_i} \|x_i^*(k|t) - x_i^a(k|t)\|_{G_j} \right. \\ &\qquad \left. + |\mathbb{A}_i \backslash \mathbb{I}_i(t+1)| \cdot \|x_i^*(k|t+1) - x_i^a(k|t+1)\|_{G_i} \right) \\ &\leqslant -\sum_{i=1}^{N} l_i(x_i^*, u_i^*, x_i^a, x_{j\in\mathbb{A}_i}^a;0|t) + \sum_{i=1}^{N}\sum_{k=1}^{N_p-1} \left(-\|x_i^*(k|t) - x_i^a(k|t)\|_{F_i} + \sum_{j\in\mathbb{B}_i} \|x_i^*(k|t) - x_i^a(k|t)\|_{G_j} \right. \\ &\qquad \left. + \frac{|\mathbb{A}_i \backslash \mathbb{I}_i(t+1)|}{\gamma_i(t+1)} \cdot \|x_i^*(k|t) - x_i^a(k|t)\|_{G_i} \right), \end{aligned} \tag{A.5}$$

where the first and second inequalities uses (A.4) and (5f), respectively.

When (8) holds, we have:

$$\begin{aligned} &\left(\sum_{j\in\mathbb{B}_i} \|x_i^*(k|t) - x_i^a(k|t)\|_{G_j} + \frac{|\mathbb{A}_i \backslash \mathbb{I}_i(t+1)|}{\gamma_i(t+1)} \cdot \|x_i^*(k|t) - x_i^a(k|t)\|_{G_i} \right)^2 \\ &\leqslant (|\mathbb{B}_i| + 1) \cdot \left(\sum_{j\in\mathbb{B}_i} \|x_i^*(k|t) - x_i^a(k|t)\|_{G_j}^2 + \left(\frac{|\mathbb{A}_i \backslash \mathbb{I}_i(t+1)|}{\gamma_i(t+1)} \right)^2 \cdot \|x_i^*(k|t) - x_i^a(k|t)\|_{G_i}^2 \right) \\ &= \|x_i^*(k|t) - x_i^a(k|t)\|^2_{(|\mathbb{B}_i|+1)\cdot\left(\sum_{j\in\mathbb{B}_i} G_j + \left(\frac{|\mathbb{A}_i \backslash \mathbb{I}_i(t+1)|}{\gamma_i(t+1)} \right)^2 \cdot G_i \right)} \\ &\leqslant \|x_i^*(k|t) - x_i^a(k|t)\|_{\bar{F}_i}^2, \end{aligned} \tag{A.6}$$

where the first and second inequalities use Lemma 2 and (8), respectively. Then we extract the square root of both sides of (A.6) and obtain:

$$\sum_{j\in\mathbb{B}_i} \|x_i^*(k|t) - x_i^a(k|t)\|_{G_j} + \frac{|\mathbb{A}_i \backslash \mathbb{I}_i(t+1)|}{\gamma_i(t+1)} \cdot \|x_i^*(k|t) - x_i^a(k|t)\|_{G_i} \leqslant \|x_i^*(k|t) - x_i^a(k|t)\|_{\bar{F}_i}. \tag{A.7}$$

By plugging (A.7) into (A.5), we have:

$$V_{\mathbb{A}}(t+1) - V_{\mathbb{A}}(t) \leqslant -\sum_{i=1}^{N} l_i(x_i^*, u_i^*, x_i^a, x_{j\in\mathbb{A}_i}^a;0|t) \leqslant 0,$$

where the equality holds if and only if

$$\begin{aligned} u_i^*(0|t) &= 0, \\ x_i^*(0|t) - x_i^a(0|t) &= 0, \\ x_i^*(0|t) - x_j^a(0|t) + \widetilde{d}_{ij} &= 0, \ \forall\, j \in \mathbb{I}_i(t), \end{aligned}$$

which corresponds to the equilibrium state of the system. Then, according to the Lyapunov theorem, the closed-loop system is asymptotically stable.

References

Bian, Y., Li, S.E., Ren, W., Wang, J., Li, K., Liu, H., 2019. Cooperation of multiple connected vehicles at unsignalized intersections: Distributed observation, optimization, and control. IEEE Trans. Industr. Electron. 1–10. https://doi.org/10.1109/TIE.2019.2960757.

Bian, Y., Zheng, Y., Ren, W., Li, S.E., Wang, J., Li, K., 2019. Reducing time headway for platooning of connected vehicles via V2V communication. Transport. Res. Part C: Emerg. Technol. 102, 87–105. https://doi.org/10.1016/j.trc.2019.03.002.

Chehardoli, H., Homaeinezhad, M., 2017. Stable control of a heterogeneous platoon of vehicles with switched interaction topology, time-varying communication delay and lag of actuator. Proc. Inst. Mech. Eng., Part C: J. Mech. Eng. Sci. 231, 4197–4208. https://doi.org/10.1177/0954406217709491.

Cheng, Z., Zhang, H.-T., Fan, M.-C., Chen, G., 2015. Distributed consensus of multi-agent systems with input constraints: A model predictive control approach. IEEE Trans. Circ. Syst. I Regul. Pap. 62, 825–834. https://doi.org/10.1109/TCSI.2014.2367575.

Darbha, S., Hedrick, J., 1999. Constant spacing strategies for platooning in Automated Highway Systems. J. Dynam. Syst. Measur. Control-Trans. ASME 121, 462–470. https://doi.org/10.1115/1.2802497.

di Bernardo, M., Falcone, P., Salvi, A., Santini, S., 2016. Design, analysis, and experimental validation of a distributed protocol for platooning in the presence of time-varying heterogeneous delays. IEEE Trans. Control Syst. Technol. 24, 413–427. https://doi.org/10.1109/TCST.2015.2437336.

di Bernardo, M., Salvi, A., Santini, S., 2015. Distributed consensus strategy for platooning of vehicles in the presence of time-varying heterogeneous communication delays. IEEE Trans. Intell. Transp. Syst. 16, 102–112. https://doi.org/10.1109/TITS.2014.2328439.

Ding, B., Ge, L., Pan, H., Wang, P., 2016. Distributed MPC for tracking and formation of homogeneous multi-agent system with time-varying communication topology. Asian J. Control 18, 1030–1041. https://doi.org/10.1002/asjc.1186.

Dunbar, W.B., Caveney, D.S., 2012. Distributed receding horizon control of vehicle platoons: Stability and string stability. IEEE Trans. Autom. Control 57, 620–633. https://doi.org/10.1109/TAC.2011.2159651.

Flores, C., Milanés, V., 2018. Fractional-order-based ACC/CACC algorithm for improving string stability. Transport. Res. Part C: Emerg. Technol. 95, 381–393. https://doi.org/10.1016/j.trc.2018.07.026.

Gao, F., Hu, X., Li, S.E., Li, K., Sun, Q., 2018. Distributed adaptive sliding mode control of vehicular platoon with uncertain interaction topology. IEEE Trans. Industr. Electron. 65, 6352–6361. https://doi.org/10.1109/TIE.2017.2787574.

Ge, J.I., Orosz, G., 2017. Optimal control of connected vehicle systems with communication delay and driver reaction time. IEEE Trans. Intell. Transp. Syst. 18, 2056–2070. https://doi.org/10.1109/TITS.2016.2633164.

Gong, S., Shen, J., Du, L., 2016. Constrained optimization and distributed computation based car following control of a connected and autonomous vehicle platoon. Transport. Res. Part B: Methodol. 94, 314–334. https://doi.org/10.1016/j.trb.2016.09.016.

Heidarinejad, M., Liu, J., de la Pena, D.M., Davis, J.F., Christofides, P.D., 2011. Handling communication disruptions in distributed model predictive control. J. Process Control 21, 173–181. https://doi.org/10.1016/j.jprocont.2010.11.005.

Khamsi, M.A., Kirk, W.A., 2011. An introduction to metric spaces and fixed point theory. John Wiley & Sonshttps://doi.org/10.1002/9781118033074.ch8.

Kwon, J.W., Chwa, D., 2014. Adaptive bidirectional platoon control using a coupled sliding mode control method. IEEE Trans. Intell. Transp. Syst. 15, 2040–2048. https://doi.org/10.1109/TITS.2014.2308535.

Li, S.E., Gao, F., Li, K., Wang, L., You, K., Cao, D., 2018a. Robust longitudinal control of multi-vehicle systems-A distributed H-infinity method. IEEE Trans. Intell. Transp. Syst. 19, 2779–2788. https://doi.org/10.1109/TITS.2017.2760910.

Li, S.E., Zheng, Y., Li, K., Wu, Y., Hedrick, J.K., Gao, F., Zhang, H., 2017. Dynamical modeling and distributed control of connected and automated vehicles: Challenges and opportunities. IEEE Intell. Transp. Syst. Mag. 9, 46–58. https://doi.org/10.1109/MITS.2017.2709781.

Li, Y., Tang, C., Li, K., Peeta, S., He, X., Wang, Y., 2018b. Nonlinear finite-time consensus-based connected vehicle platoon control under fixed and switching communication topologies. Transport. Res. Part C: Emerg. Technol. 93, 525–543. https://doi.org/10.1016/j.trc.2018.06.013.

Liberzon, D., 2003. Switching in systems and control. Birkhauser, Boston. https://doi.org/10.1007/978-1-4612-0017-8.

Lioris, J., Pedarsani, R., Tascikaraoglu, F.Y., Varaiya, P., 2017. Platoons of connected vehicles can double throughput in urban roads. Transport. Res. Part C: Emerg. Technol. 77, 292–305. https://doi.org/10.1016/j.trc.2017.01.023.

Liu, P., Kurt, A., Ozguner, U., 2019. Distributed model predictive control for cooperative and flexible vehicle platooning. IEEE Trans. Control Syst. Technol. 27, 1115–1128. https://doi.org/10.1109/TCST.2018.2808911.

Petrillo, A., Salvi, A., Santini, S., Valente, A.S., 2018. Adaptive multi-agents synchronization for collaborative driving of autonomous vehicles with multiple communication delays. Transport. Res. Part C: Emerg. Technol. 86, 372–392. https://doi.org/10.1016/j.trc.2017.11.009.

Ploeg, J., Shukla, D.P., van de Wouw, N., Nijmeijer, H., 2014. Controller synthesis for string stability of vehicle platoons. IEEE Trans. Intell. Transp. Syst. 15, 854–865. https://doi.org/10.1109/TITS.2013.2291493.

Ploeg, J., van de Wouw, N., Nijmeijer, H., 2014. L-p string stability of cascaded systems: Application to vehicle platooning. IEEE Trans. Control Syst. Technol. 22, 786–793. https://doi.org/10.1109/TCST.2013.2258346.

Rödönyi, G., 2018. An adaptive spacing policy guaranteeing string stability in multi-brand ad hoc platoons. IEEE Trans. Intell. Transp. Syst. 19, 1902–1912. https://doi.org/10.1109/TITS.2017.2749607.

Salvi, A., Santini, S., Valente, A.S., 2017. Design, analysis and performance evaluation of a third order distributed protocol for platooning in the presence of time-varying delays and switching topologies. Transport. Res. Part C: Emerg. Technol. 80, 360–383. https://doi.org/10.1016/j.trc.2017.04.013.

Schaich, R.M., Müller, M.A., Allgöwer, F., 2014. A distributed model predictive control scheme for networks with communication failure. IFAC Proc. Volumes 47, 12004–12009. https://doi.org/10.3182/20140824-6-za-1003.01507.

Seiler, P., Pant, A., Hedrick, K., 2004. Disturbance propagation in vehicle strings. IEEE Trans. Autom. Control 49, 1835–1842. https://doi.org/10.1109/TAC.2004.835586.

Shladover, S.E., 2007. PATH at 20 - History and major milestones. IEEE Trans. Intell. Transp. Syst. 8, 584–592. https://doi.org/10.1109/TITS.2007.903052.

Shladover, S.E., Desoer, C.A., Hedrick, J.K., Tomizuka, M., Walrand, J., Zhang, W.-B., McMahon, D.H., Peng, H., Sheikholeslam, S., McKeown, N., 1991. Automated vehicle control developments in the PATH program. IEEE Trans. Veh. Technol. 40, 114–130. https://doi.org/10.1109/25.69979.

Steele, J.M., 2004. The Cauchy-Schwarz master class: An introduction to the art of mathematical inequalities. Cambridge University Presshttps://doi.org/10.1017/CBO9780511817106.

Talebpour, A., Mahmassani, H.S., 2016. Influence of connected and autonomous vehicles on traffic flow stability and throughput. Transport. Res. Part C: Emerg. Technol. 71, 143–163. https://doi.org/10.1016/j.trc.2016.07.007.

Wang, C., Gong, S., Zhou, A., Li, T., Peeta, S., 2020a. Cooperative adaptive cruise control for connected autonomous vehicles by factoring communication-related constraints. Transport. Res. Part C: Emerg. Technol. 113, 124–145. https://doi.org/10.1016/j.trc.2019.04.010.

Wang, M., 2018. Infrastructure assisted adaptive driving to stabilise heterogeneous vehicle strings. Transport. Res. Part C: Emerg. Technol. 91, 276–295. https://doi.org/10.1016/j.trc.2018.04.010.

Wang, M., Daamen, W., Hoogendoorn, S.P., van Arem, B., 2016. Cooperative car-following control: Distributed algorithm and impact on moving jam features. IEEE Trans. Intell. Transp. Syst. 17, 1459–1471. https://doi.org/10.1109/TITS.2015.2505674.

Wang, P., Feng, X., Li, W., Yu, W., 2017. DRHC synthesis for simultaneous tracking and formation of nonhomogeneous multi-agents with time-varying communication topology. Int. J. Adv. Rob. Syst. 14, 1–15. https://doi.org/10.1177/1729881416658177.

Wang, Z., Bian, Y., Shladover, S.E., Wu, G., Li, S.E., Barth, M.J., 2020b. A survey on cooperative longitudinal motion control of multiple connected and automated vehicles. IEEE Intell. Transp. Syst. Mag. 12, 4–24. https://doi.org/10.1109/MITS.2019.2953562.

Xiao, L., Gao, F., 2011. Practical string stability of platoon of adaptive cruise control vehicles. IEEE Trans. Intell. Transp. Syst. 12, 1184–1194. https://doi.org/10.1109/TITS.2011.2143407.

Xu, B., Ban, X.J., Bian, Y., Li, W., Wang, J., Li, S.E., Li, K., 2019. Cooperative method of traffic signal optimization and speed control of connected vehicles at isolated intersections. IEEE Trans. Intell. Transp. Syst. 20, 1390–1403. https://doi.org/10.1109/TITS.2018.2849029.

Xu, B., Li, S.E., Bian, Y., Li, S., Ban, X.J., Wang, J., Li, K., 2018. Distributed conflict-free cooperation for multiple connected vehicles at unsignalized intersections. Transport. Res. Part C: Emerg. Technol. 93, 322–334. https://doi.org/10.1016/j.trc.2018.06.004.

Yu, S.-M., Wu, S.-N., Zhao, Y.-B., He, D.-F., 2018. Delayed feedback mpc algorithms of vehicle platoons subject to constraints on measurement range and driving behaviors. Asian J. Control 20, 2260–2270. https://doi.org/10.1002/asjc.1761.

Zhan, J., Li, X., 2013. Consensus of sampled-data multi-agent networking systems via model predictive control. Automatica 49, 2502–2507. https://doi.org/10.1016/j.automatica.2013.04.037.

Zhang, L., Orosz, G., 2016. Motif-based design for connected vehicle systems in presence of heterogeneous connectivity structures and time delays. IEEE Trans. Intell. Transp. Syst. 17, 1638–1651. https://doi.org/10.1109/TITS.2015.2509782.

Zheng, Y., Bian, Y., Li, S., Li, S.E., 2019. Cooperative control of heterogeneous connected vehicles with directed acyclic interactions. IEEE Intell. Transp. Syst. Mag. 1–16. https://doi.org/10.1109/MITS.2018.2889654.

Zheng, Y., Li, S.E., Li, K., Borrelli, F., Hedrick, J.K., 2017. Distributed model predictive control for heterogeneous vehicle platoons under unidirectional topologies. IEEE Trans. Control Syst. Technol. 25, 899–910. https://doi.org/10.1109/TCST.2016.2594588.

Zheng, Y., Li, S.E., Wang, J., Cao, D., Li, K., 2016. Stability and scalability of homogeneous vehicular platoon: Study on the influence of information flow topologies. IEEE Trans. Intell. Transp. Syst. 17, 14–26. https://doi.org/10.1109/TITS.2015.2402153.

Zhou, J., Peng, H., 2005. Range policy of adaptive cruise control vehicles for improved flow stability and string stability. IEEE Trans. Intell. Transp. Syst. 6, 229–237. https://doi.org/10.1109/TITS.2005.848359.

Zhou, Y., Wang, M., Ahn, S., 2019. Distributed model predictive control approach for cooperative car-following with guaranteed local and string stability. Transport. Res. Part B: Methodol. 128, 69–86. https://doi.org/10.1016/j.trb.2019.07.001.